Biosensors and Bioelectronics 93 (2017) 241–249

Contents lists available at ScienceDirect

Biosensors and Bioelectronics

journal homepage: www.elsevier.com/locate/bios

Monitoring the electrochemical responses of neurotransmitters through localized surface plasmon resonance using nanohole array

Nantao Li [a,b], Yanli Lu [a,b], Shuang Li [a], Qian Zhang [a], Jiajia Wu [a], Jing Jiang [c], Gang Logan Liu [c], Qingjun Liu [a,b,*]

[a] Biosensor National Special Laboratory, Key Laboratory for Biomedical Engineering of Education Ministry, Department of Biomedical Engineering, Zhejiang University, Hangzhou, 310027 PR China
[b] Collaborative Innovation Center of TCM Health Management, Fujian University of Traditional Chinese Medicine, Fuzhou, 350122 PR China
[c] Micro and Nanotechnology Lab, University of Illinois at Urbana-Champaign, IL, 61801 USA

ARTICLE INFO

Article history:
Received 17 June 2016
Received in revised form
17 August 2016
Accepted 29 August 2016
Available online 30 August 2016

Keywords:
Coupled detection
Localized surface plasmon resonance (LSPR)
Cyclic voltammetry (CV)
Spectroelectrochemistry
Neurotransmitters

ABSTRACT

In this study, a novel spectroelectrochemical method was proposed for neurotransmitters detection. The central sensing device was a hybrid structure of nanohole array and gold nanoparticles, which demonstrated good conductivity and high localized surface plasmon resonance (LSPR) sensitivity. By utilizing such specially-designed nanoplasmonic sensor as working electrode, both electrical and spectral responses on the surface of the sensor could be simultaneously detected during the electrochemical process. Cyclic voltammetry was implemented to activate the oxidation and recovery of dopamine and serotonin, while transmission spectrum measurement was carried out to synchronously record to LSPR responses of the nanoplasmonic sensor. Coupling with electrochemistry, LSPR results indicated good integrity and linearity, along with promising accuracy in qualitative and quantitative detection even for mixed solution and in brain tissue homogenates. Also, the detection results of other negatively-charged neurotransmitters like acetylcholine demonstrated the selectivity of our detection method for transmitters with positive charge. When compared with traditional electrochemical signals, LSPR signals provided better signal-to-noise ratio and lower detection limits, along with immunity against interference factors like ascorbic acid. Taking the advantages of such robustness, the coupled detection method was proved to be a promising platform for point-of-care testing for neurotransmitters.

1. Introduction

Neurotransmitters are chemicals released by central and peripheral neural system that allow for signal transmission among neurons, and could be categorized into two types: excitatory neurotransmitters like dopamine, and inhibitory neurotransmitters like serotonin. These neurotransmitters are substantial in maintaining normal neurological functionalities, for example, dopamine in normal range allows the ordinary freedom of movement whereas insufficient dose of dopamine could trigger Parkinson's disease and schizophrenia (Arreguin et al., 2009). Serotonin, on the other hand, is responsible for balancing excessive excitatory neurotransmitters. Abnormal level of serotonin could trigger carcinoid syndrome (Wright-Honari et al., 1990) and depression (Mahar et al., 2014). Therefore, the accurate, real-time and on-spot measurement of these neurotransmitters are crucial not only in unraveling the mechanisms of neurological diseases but also in preventing possible neural disorders. Currently traditional detection methods are still widely used in neurotransmitters detection, such as capillary electrophoresis (Voegel et al., 1997; Zhou et al., 1995), fluorescence spectrometry (Clarke et al., 2008; Pérez-Ruiz et al., 2007; Wu et al., 2007) and liquid chromatography (Uutela et al., 2008). These detection techniques, however, are either time-consuming or expensive, requiring bulky detection equipment and complicated biomaterial binding process. To meet with the instantaneity and low-cost requirements of point-of-care (POC) monitoring neurotransmitters, several methods had been further developed, including electrochemical detection (Robinson et al., 2003) and nanoplasmonic sensing (Qin et al., 2015; Zheng et al., 2011).

Electrochemistry provides label-free methods to determine concentration and to yield energy data through redox potentials, and could be miniaturized using microelectronics technologies.

* Corresponding author at: Biosensor National Special Laboratory, Key Laboratory for Biomedical Engineering of Education Ministry, Department of Biomedical Engineering, Zhejiang University, Hangzhou 310027, PR China.
E-mail address: qjliu@zju.edu.cn (Q. Liu).

http://dx.doi.org/10.1016/j.bios.2016.08.105
0956-5663/

Therefore it has been extensively utilized, especially for cyclic voltammetry, in rapid, on-spot determination of neurotransmitters, both in vivo (O'Neill, 1994) and in vitro (Mark et al., 1995). However, since the internal biological environments are extremely complicated, containing various kinds of interfering substances like ascorbic acid that always coexists with trace dopamine in organisms and shares a similar oxidation potential, therefore it is extremely difficult for direct examination using electrochemistry. Mostly in these electrochemical techniques, specially-designed electrodes were utilized in detection of neurotransmitters in order to both increase the sensitivity, selectivity as well as enhancing adsorption for trace transmitters (Ali et al., 2007; Sun et al., 2009). Unfortunately, the modification of electrode surface usually suffer from quick sensitivity loss and signal instability, like the electrochemically decorated electrodes reported in several publications (Gonon et al., 1981; Hafizi et al., 1990). In addition, one of the most commonly used electrochemical techniques, fast cyclic voltammetry, usually suffer from dramatic signal contortion and background noises, which increased the difficulty for accurate quantitative determination of neurotransmitters (Hermans et al., 2008).

The other promising detection method for neurotransmitters and other molecules is nanoplasmonic sensing. Plasmonic sensing is an enabling optical technique with capabilities of high-sensitive surface condition monitoring. Among nanoplasmonic sensing techniques, localized surface plasmon resonance (LSPR) sensing relies on localized field enhancement and confinement in close proximity to nanoparticles and therefore require very limited space for sensing (Willets and Van Duyne, 2007). In accordance with interface condition especially refractive index changes on the surface, LSPR could be triggered between the incident light and the surface plasmon, and resulting in corresponding change in transmission spectrum. Numerous effort have been placed on utilizing LSPR sensing methods to detect neurotransmitters, and most of these sensing methods are based on immunoassay in order to obtain specificity (Zhao et al., 2008). These methods, although generally granted with high sensitivity and promising selectivity, usually require complicated surface decoration process and therefore have limited repeatability because bioactive material are very fragile. Therefore, LSPR sensing are still limited in POC testing.

Hereby we proposed a spectroelectrochemical sensing method for the detection of neurotransmitters, i.e., to combine cyclic voltammetry and LSPR measurement for studying the redox chemistry of neurotransmitters. The experiment was based on a previously-reported nanohole array sensing device (Gartia et al., 2013; Zhang et al., 2015), namely the Lycurgus nanocup array, which was utilized as working electrode. Oxidation states of dopamine and serotonin, at the presence of ascorbic acid, were changed electrochemically by addition or removal of electrons at the surface of the nanostructured electrode, while spectral measurement was simultaneously carried out to record the refractive index changes of the solution adjacent to the electrode. Results from both electrochemical and LSPR dimensions demonstrated good integrity, and LSPR results were shown to be immune against interference like pH value, buffer solution and ascorbic acid. The specificity of the coupled detection method was tested by analyzing mixed solution of dopamine, serotonin and ascorbic acid as well as acetylcholine and uric acid. Finally dopamine and serotonin was detected in rat brain tissue homogenates, and the accuracy of LSPR remained promising. Our robust detection system requires no biomaterial decoration and have the potential for miniaturization, therefore could potentially be further developed into a low-cost point-of-care platform for in vitro neurotransmitter monitoring.

2. Experiment

2.1. Reagents and materials

Tetrachloroauric(III) acid hydrate, potassium ferricyanide ($K_3Fe(CN)_6$), potassium ferrocyanide ($K_4Fe(CN)_6$), dopamine hydrochloride, serotonin hydrochloride, ascorbic acid, acetylcholine, uric acid and artificial cerebrospinal fluid (aCSF) were purchased directly from Sigma-Aldrich (Oakville, ON). All other chemicals were of analytical grade and were used as received. Sprague-Dawley rats with weights of 250 g to 300 g purchased from the Laboratory of Animal Research Center (Zhejiang Province, China).

Stock solutions of dopamine and serotonin were prepared by dissolving transmitters in the phosphate buffer saline (PBS, pH=7.2), and were diluted to desired concentrations before use. Preparation of rat brain tissue homogenates was include in Appendix A. All solutions were stored at 4 °C and protected from light.

2.2. Nanosensor fabrication

Replica molding technique was utilized in this study to reduce fabrication cost. The master nanocone array (nanocone height was 500 nm, and pitch 350 nm, periodicity 350 nm) was fabricated on the glass substrate using the laser interference lithography patterning and reaction ion etching technique, followed by cleaning and silanizing with dimethyl dichlorosilane solution for 30 min and rinsing in ethanol and deionized water. Then, as indicated in Fig. 1a, the two-dimensional square lattice was transferred to a flexible and optically transparent polydimethylsiloxane (PMDS) film using nanoreplica molding process: 5 μL of UV-curable polymer (NOA-61) was evenly spread on the top of the nanocone master and a PET sheet of 250 μm thick was carefully put on top of the polymer, to avoid the bubble formation and to act as a substrate. The UV polymer was cured with a UV light-curing flood lamp system (Dymax EC-Series) with average power density of 105 mW/cm^2 for 60 s at room temperature, after which the nanopatterned PET substrate was peeled off carefully from the master mold (Fig. 1b). In order to make the structure surface plasmon active, a thin adhesive layer of Titanium (5 nm) was deposited and followed by 90 nm of metal layer of gold (Fig. 1c).

As seen in Fig. 1d, in order to enhance the optical and electrochemical properties of the electrode, AuNPs were galvanized onto the nanostructured surface by applying cyclic voltammetry (scope −0.6 V −1.5 V, scan rate=0.1 V/s) in chloroauric acid (1 wt%) in the standard three-electrode system where the gold working electrode was replaced with the fabricated nanostructured sensor. Scanning cycles of CV was optimized as 1 cycle according to the optical responses of the galvanized electrode against dopamine (Appendix B depicted the LSPR responses of the nanosensor with different cycles of galvanization CV). Finally the fabricated nanohole array was trimmed into 2 mm × 4 mm strips and employed as working electrodes.

2.3. Detection system

The coupled measuring system is comprised of two components, i.e., the LSPR monitoring system and the electrochemical measuring system.

For the LSPR monitoring system, a halogen cold light source (DT-MINI-2, Ocean Optics Inc., Dunedin, USA) was utilized as light source, whilst a spectrophotometer receptor (USB2000+, Ocean Optics Inc., Dunedin, USA) was used to record the transmission spectrum of the nanostructured electrode. A light emitting probe and a light receptor probe were connected to the light source and the spectrophotometer respectively by fiber bundles and allowed

for regional illumination and transmission spectrum recording. Both the emitting probe and the receptor probe are immobilized with optical brackets, and vertically placed 1 cm away from the electrochemical reactor chamber. Collimating lens was utilized to ensure the light path is vertical straight.

On the other hand, the electrochemical measuring system included a standard three-electrode system and a perfusion system. Instead of using traditional gold electrode for working electrode (WE), the nanosensor device was utilized as working electrode whilst platinum electrode and Ag/AgCl electrode were used as counter-electrode (CE) and reference electrode (RE). Original electrochemical data and primary data processing were based on electrochemical workstation (CHI660E, Chenhua, China). The two detection systems were aligned by an external trigger, which allowed for simultaneous beginning of both detection processes.

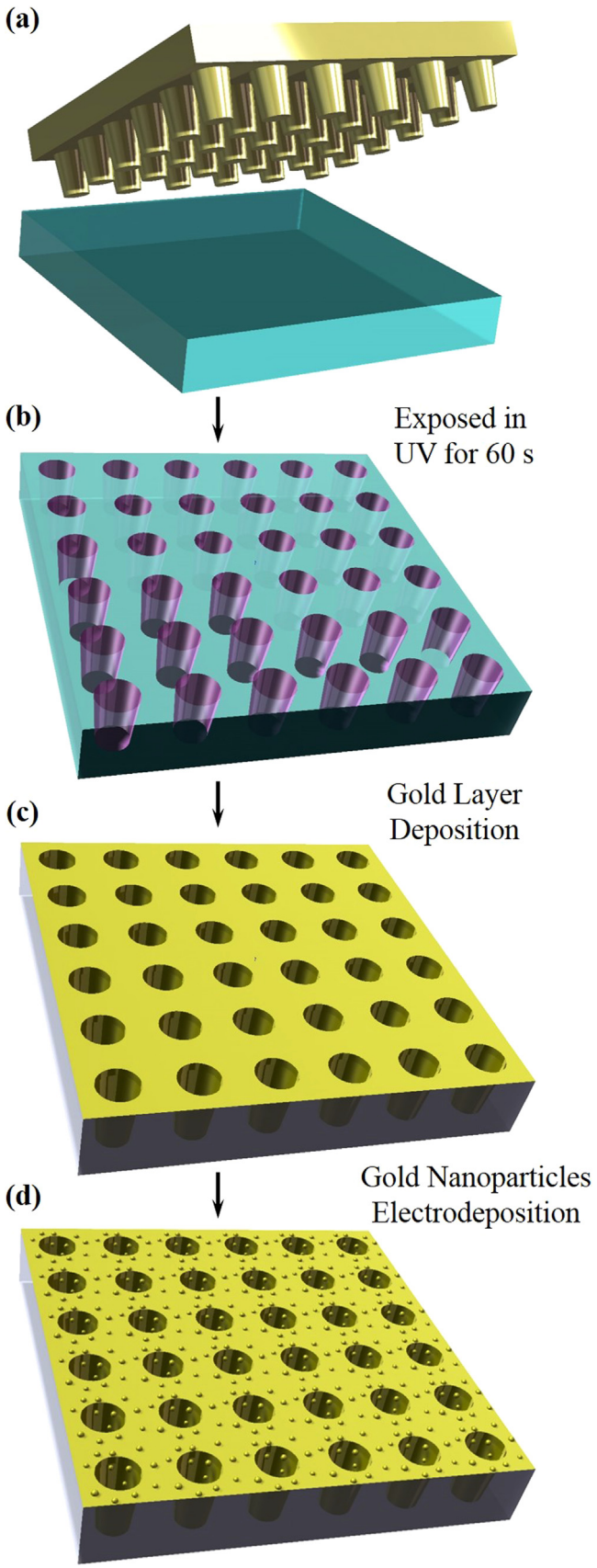

Fig. 1. Fabrication process of the optical-electrochemical nanosensor. (a) Glass nanocone array was fabricated using laser interference lithography patterning and used as master film for nanoimprinting. (b) Imprinted by nanocone array, the UV-curable polymer substrate was exposed in UV for 60 s before removing the master film, and the two-dimensional square lattice was transferred onto the PET substrate. (c) The nanohole array was then deposited with a thin adhesive layer of Titanium (5 nm) and followed gold layer with thickness of 90 nm. (d) Finally the nanostructured surface was galvanized with AuNPs (diameter of ~50 nm) to enhance its sensitivity.

2.4. Spectroelectrochemical detection for neurotransmitters

Using the coupled measuring system, the optical and electrochemical detection for neurotransmitters could be implemented simultaneously. Stock solution of dopamine and serotonin were diluted by PSB solution to desired concentrations (5 μmol/L, 25 μmol/L, 50 μmol/L, 75;μmol/L and 100 μmol/L), and then loaded into the electrochemical reaction chamber before conducting the LSPR-CV detection process. For CV detection of dopamine and serotonin, the scope ranged from −0.4 V to 1.0 V, with scan rate set to be 0.01 V/s as reported in previous publications. Five complete CV cycles were conducted consecutively in each complete detection in order to observe the decay of signal as CV cycles increase, and therefore the entire CV detection process lasted for 1400 s. Whilst the CV was performed, the spectrophotometer, as mentioned previously, recorded the transmission spectrum on the surface of the nanoplasmonic sensor every second. The recorded transmission spectrum ranges from 300 nm to 1000 nm with 0.2 nm increment.

3. Results and discussion

3.1. Optical and electrochemical characterization of the nanosensor

Fig. 2 demonstrates the detailed microscale morphology of the nanocone array mold and the nanostructured electrode, along with its optical and electrochemical properties. The field-emission scanning electron microscopy (FE-SEM) images of Fig. 2a revealed that by the virtue of laser interference lithography, the nanocone structure was successfully etched on the surface of the glass substrate. The diameter of each holes in Fig. 2b was 100 nm. As seen in Fig. 2b, dense layer of AuNPs (average diameter: ~50 nm) were electroplated onto the entire surface of the nanosensor, including the sidewalls. Basing on a report that elucidated the dominant role of in-hole gold layers in the peak shift for plasmonic sensing (Ferreira et al., 2008), AuNPs were electroplated to further enhance the sensitivity of our nanosensor (preliminary experiments had indicated that without electroplated AuNPs, LSPR during the electrochemical process could barely be observed).

Optical and electrochemical characterization were carried out by recording the transmission spectrum (Fig. 2c) and cyclic voltammogram (Fig. 2d) in 25 mmol/L $Fe(CN)_6^{3-}/^{4-}$ solution (scope: −0.2 to 0.6 V, scan rate: 0.1 V/s). As shown in Fig. 2c, the

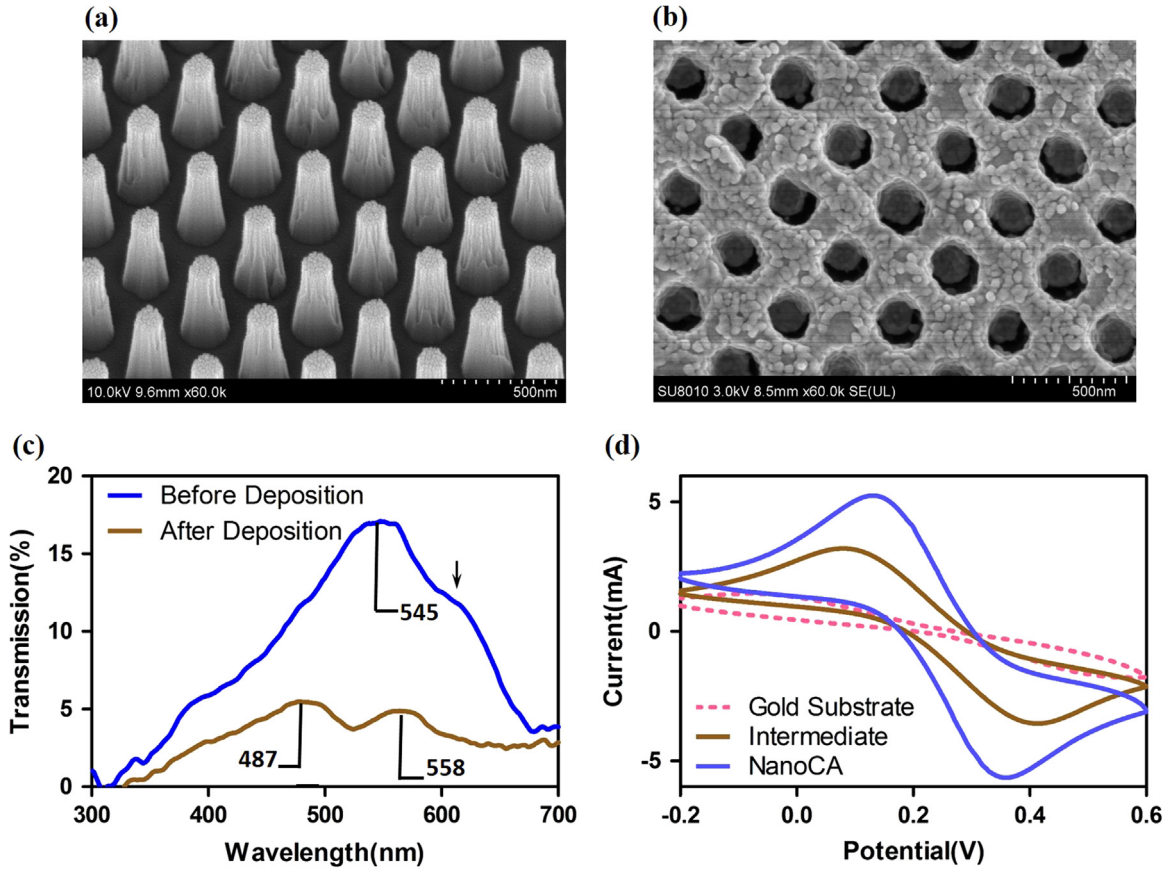

Fig. 2. Characterizations of the fabricated nanocone array and nanosensor. (a) SEM image of glass nanocone array, uniform nanocone structures with periodicity of 350 nm. (b) SEM image of the fabricated nanosensor. Evenly distributed AuNPs could be seen on the surface and the sidewall of the nanohole structure. (c) Transmission spectrum of the nanosensor before and after AuNPs deposition. It can be seen in the spectrum that with the addition of AuNPs, another characteristic peak appeared at 558 nm, and might be traced back to the shoulder of the original transmission spectrum as marked with arrow. (d) Cyclic voltammogram of different films in redox pair of $K_3Fe(CN)_6$ and $K_4Fe(CN)_6$. Results indicated that the deposited AuNPs could dramatically enhance the conductivity of the sensing device.

deposition of gold layer activated the surface plasmon, providing a major characteristic peak in the transmission spectrum. With the AuNPs electroplated on sidewalls, the transmission of the electrode dropped significantly and demonstrated hypsochromic shift for the characteristic transmission peak with the addition of a new transmission peak (colorimetric changes of the electrode after galvanization could be observed by naked eye, Appendix C is the photo indicating such colorimetric change). According to previous publication (Gartia et al., 2013), the second transmission peak at 558 nm was due to the scattering from AuNPs in PET environment ($n=1.56$).

For the electrochemical properties of the fabricated nanosensor, Fig. 2d depicted the cyclic voltammograms of working electrodes with different structures: plain PET substrate coated with gold layer, the intermediate product of nanosensor fabrication (i.e. the nanohole array structure was transferred on the PET substrate and deposited with gold layer, but without AuNPs deposited) and the final nanosensor. It can be clearly observed from the voltammograms that the anodic and cathodic current of nanosensor was much higher than the rest of the devices, which demonstrated the important role of the hybrid structure of nanosensor and AuNPs in enhancing the conductivity of the entire device.

3.2. *Plasmonic responses of transmitters during electrochemical process*

Cyclic voltammogram could provide quantitatively the thermodynamics of redox processes and the kinetics of heterogeneous electron transfer reactions (Kawagoe et al., 1993), and the characteristic current peaks in the voltammogram are considered to be related to the oxidation and recovery of many electroactive substances (Evans et al., 1983; Wang, 2006), which in our case were dopamine and serotonin. Therefore, the cyclic voltammogram of dopamine was initially used for allocating the oxidation of dopamine on the electrode in time domain, and furthermore for the collimation of the corresponding plasmonic responses.

In Fig. 3a, using nanosensor as the working electrode, the typical cyclic voltammogram of dopamine (100 μmol/L) in PBS solution was shown, and oxidation current of dopamine occurred at ~0.17 V (vs Ag/AgCl), as reported by other researchers (Wang et al., 2003; Wu et al., 2003). As cycles of CV increased, the amount of electrooxidized dopamine increased, resulting in the loss of the concentration and therefore contributed to the decreased anodic current as seen in the inset. To better clarify the location of the oxidation peaks, the cyclic voltammogram was presented in an unraveled manner: since the scanning potential varies linearly with time, the horizontal axis of Fig. 3a could also be thought as a time axis, and therefore was unfolded in time domain, as presented in Fig. 3b. The arrows allocated the location of dopamine's electrooxidation in time (first anodic peak appeared at 55 s, with the following peaks separated by ~280 s).

As mentioned previously in Section 2, the responses of LSPR on the surface of nanosensor during the electrochemical process were monitored. Fig. 3c shows several typical transmission spectra during such process: at the beginning when no electrical waveform was applied, there were two major characteristic peaks appeared on the transmission spectrum, resting on 487 nm and 558 nm respectively, and as the potential waveform (usually a

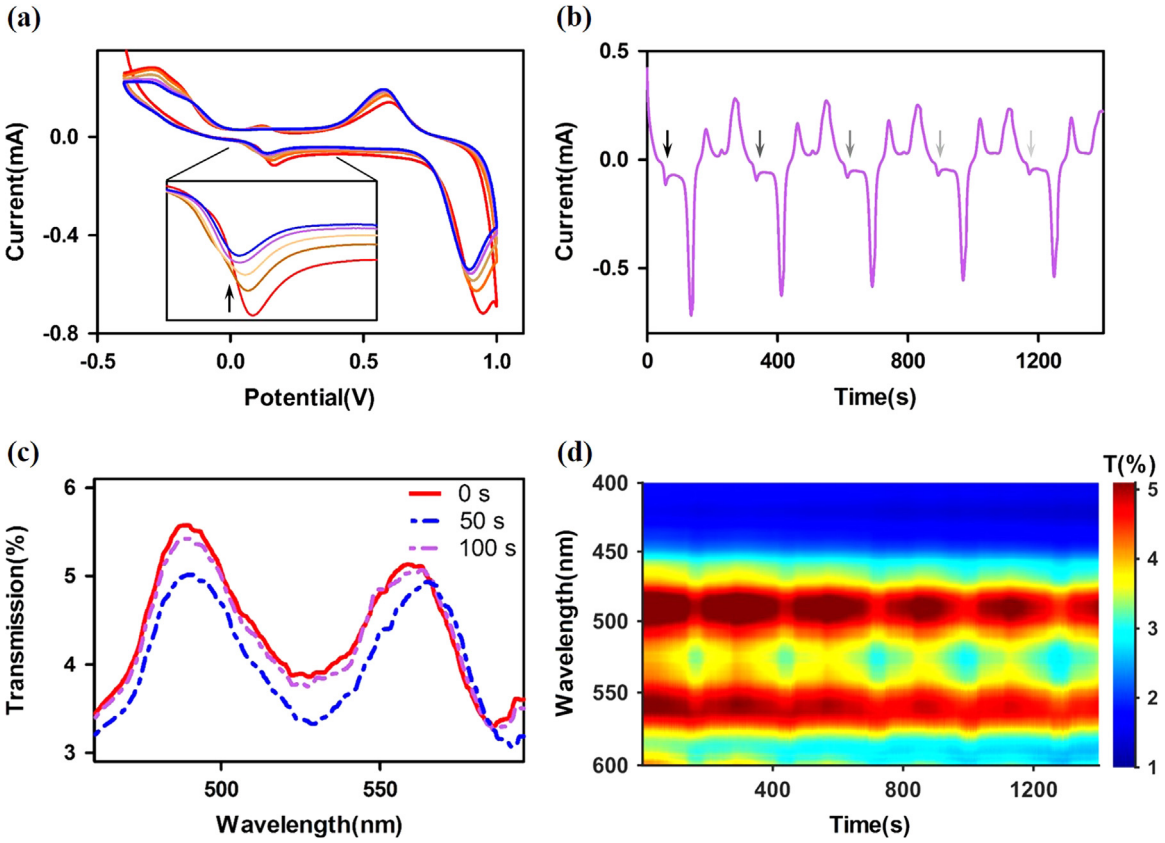

Fig. 3. Spectroelectrochemical responses of dopamine during CV. (a) Typical cyclic voltammogram of dopamine (100 μmol/L). The anodic currents (inset) was attenuated as cycles of CV increased, indicating the consumption of dopamine in the solution, as marked with arrow. (b) CV current unraveled in time domain. Anodic currents was marked with fading arrows, implying the attenuated current intensity. (c) Transmission spectrum of the nanosensor at typical moments. When anodic current occurred, significant bathochromic shift was observed for the second transmission peak, which recovered when anodic current ended. (d) Spectral responses of the nanosensor as the function of scanning time. The two transmission peaks could be observe to have periodical changes as anodic current occurred. Also the red regions faded gradually as cycles of CV increased, which is in accordance with the attenuated anodic currents. (For interpretation of the references to color in this figure legend, the reader is referred to the web version of this article.)

triangular waveform) of CV was applied, the transmission of nanosensor dropped significantly, along with the bathochromic shift (about 6 nm maximum) of second characteristic peak. To better observe the change (both intensity changes and peak position) of the transmission spectrum during CV, the color contour plot of Fig. 3d was presented by aligning every transmission spectrum as a function of time. As observed from the contour plot, the intensity of both characteristic peaks of nanosensor fluctuated periodically as the waveform developed, and the transmission intensity reached its maximum approximately when anodic current of dopamine appeared. Interestingly, the periodic red region in the contour plot shrank as CV cycles increased, verifying the consumption of dopamine in the analyte solution. As for the peak position variation, only the second transmission peak was observed to have significant periodical bathochromic shifts during CV, and therefore was used in the following sections as the major indicator for further detailed analysis.

3.3. Spectroelectrochemical behaviors of dopamine and serotonin

In order to excavate the difference of LSPR responses between neurotransmitters, aqueous dopamine and serotonin (50 μmol/L)

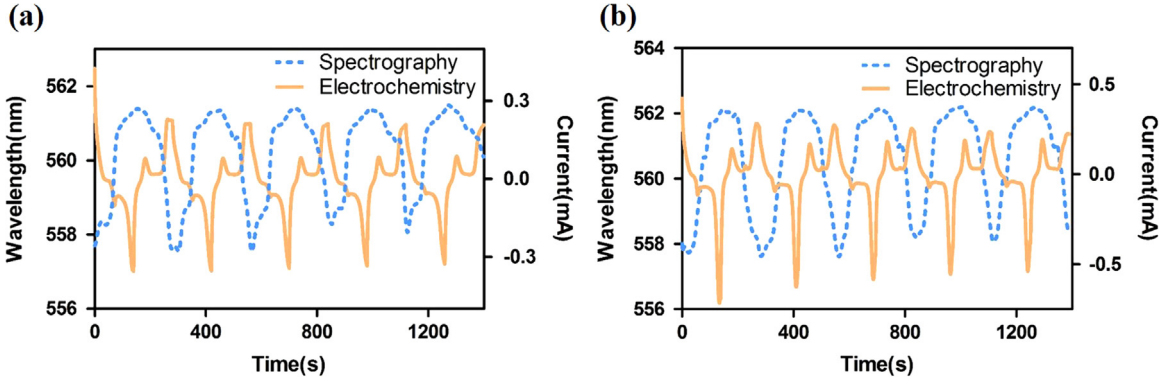

Fig. 4. LSPR and electrochemical responses of dopamine (a) and serotonin (b) during CV. For both neurotransmitters (the concentration are both 50 μmol/L), significant bathochromic shift of the second transmission peak generally concurred with the anodic current. In addition, the bathochromic shifts recovered as the scanning potential reached the switching points.

were loaded respectively into the dual detection system, where spectroelectrochemical detections were performed, as demonstrated in Section 2.4. As mentioned in the previous section, the second transmission peak was observed to have significant and periodic bathochromic shift during the CV process of dopamine, therefore was selected as the indicator for neurotransmitters behavior with respect to LSPR responses. The spectroelectrochemical responses of the two neurotransmitters, i.e., the CV current and second transmission peak position variation, were shown in Fig. 4 as the functions of scanning time.

From Fig. 4a and b, similar response patterns were observed for both CV and LSPR with respect to dopamine and serotonin. For both neurotransmitters, the anodic currents concurred with the dramatic bathochromic shifts (4.1 nm for dopamine and 3.4 nm for serotonin) of the second transmission peak, whilst the recoveries of peak position concurred approximately with the cathodic currents. In addition, generally the turning points of peak position variation curves occurred at the switching points of CV curves. Such correlation between the electrochemical and LSPR responses demonstrated that the LSPR response might serve as an alternative signal for analyte detection. Another phenomenon worth noticing is that, for both neurotransmitters, as the cycle of CV increased, the extent of bathochromic shifts was attenuated in accordance with the decreasing anodic currents.

Possible explanation of such correlation could be traced back to the mechanism of CV process (Wang, 2006): the characteristic peaks in the cyclic voltammogram resulted from the formation of the diffusion layer (or Gouy layer) near the WE surface, which is basically composed of charged molecules attracted to the surface via the Coulomb force with respect to their oxidation potentials (Compton and Banks, 2007). The thickness of diffusion layer, according to published reports (Compton and Banks, 2007; Engstrom et al., 1986; Streeter et al., 2008), varies from 10 nm to several microns depending on the structure of the electrode as well as the electrolyte. The formation of diffusion layer changes the concentration of reactant near the electrode surface, resulting in changes of refractive index in such region. According to previous publications (Chen et al., 2008; Gartia et al., 2013), the LSPR shift could be observed in the transmission spectrum when the refractive index of medium near the sensor surface was changed. Therefore by utilizing LSPR sensor as working electrode in the electrochemical process, the formation of diffusion layer could not only be monitored in cyclic voltammogram, but also be observed from LSPR signal.

3.4. Comparison of electrochemical and optical responses

Since the LSPR responses and the anodic/cathodic currents are the same phenomenon, i.e., the electrooxidation and recovery of transmitters in electrolyte, in two different dimension, therefore comparisons between these two kinds of signals were then made in order to demonstrate the advantages of LSPR-coupled detection.

The coupled detection experiments for dopamine and serotonin under gradient concentrations were carried out in order to establish correlation between neurotransmitter concentration and the corresponding LSPR shifts, and the results were depicted in Fig. 5 (each measurement of both methods in all the five concentrations was repeated five times under the same condition). Statistics indicated that, for both dopamine and serotonin, good linearity was established between LSPR shift and transmitter concentration, and Appendix D demonstrated the quality of linearity. It's worth noticing that the sensitivity of dopamine in both electrochemical signal and LSPR responses was generally higher than that of serotonin. Such phenomenon might mainly be ascribed to the higher acid dissociation constant value (pK_a) of dopamine (pK_a=8.93) (Creese et al., 1976) than that of serotonin (pK_a=4.9) (Kawashima and Kanehisa, 2000; Pratuangdejkul et al., 2006; Taylor et al., 1986), which indicated that dopamine was more electrostatically attractive to AuNPs on the surface of the working electrode. Such agreement of sensitivity in both detection methods also revealed the reliability of LSPR signal in determining the concentration of neurotransmitters.

Besides linearity, the limit of detection (LOD) and signal to noise ratio (SNR) of the two detection methods were also examined. LOD for CV detection and LSPR measurement were calculated with the 3δ/slope formula, whilst the SNR of both methods were derived according to the definition: the ratio of mean to standard deviation of the signal. The derived results were shown as followed: for traditional CV detection, LODs were calculated as 14.86 μmol/L for dopamine and 22.52 μmol/L for serotonin, and average SNRs were 21.77 and 28.52 respectively; for LSPR measurement, LODs results were 12.45 μmol/L for dopamine and 10.61 μmol/L for serotonin, and SNRs were derived as 15.74 and 15.30 respectively. The results above indicated a generally better stability and higher SNR of LSPR measurement compared with sole CV detection.

The better performance of LSPR signal might be ascribed to the lower requirement of detection environment in compared with that of electrochemical measurement. Generally in an electrochemical measurement process, the electrolyte conditions could be calibrated repeatedly before formal measurement. For instance,

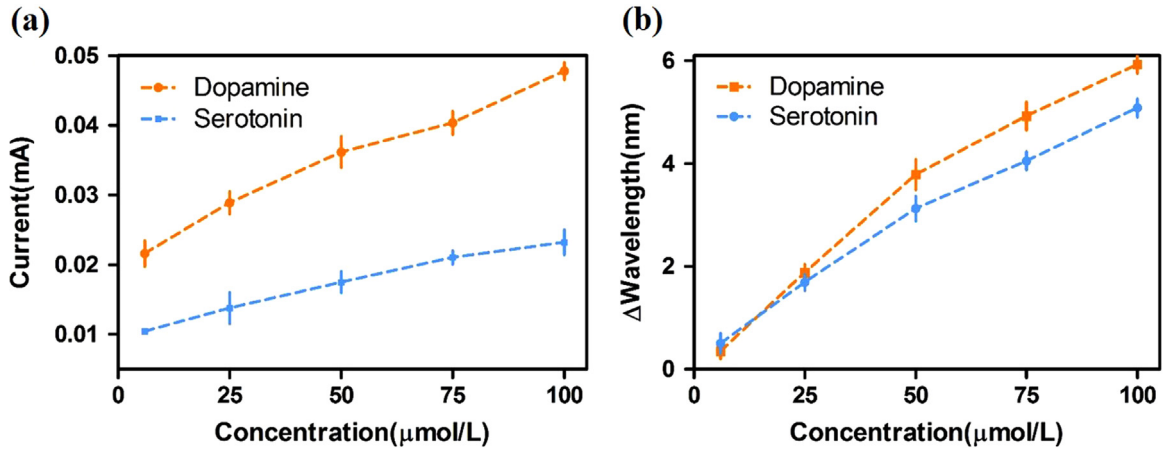

Fig. 5. Calibration plot of anodic current (a) and transmission peak position variation (b) versus neurotransmitters concentrations (i.e., 10 μmol/L, 25 μmol/L, 50 μmol/L, 75 μmol/L, 100 μmol/L).

the buffer solution and pH value of the reactant could influence the final results dramatically by introducing background current and weakening the peak height in the cyclic voltammogram (Baldrianova et al., 2011). Other artifacts such as the reduction of dissolved oxygen and evolution of hydrogen could also contort the anodic currents (Wang, 1985; Wang et al., 2007). In contrast, LSPR signal were supposed to be immune to these artifacts, since LSPR are mainly sensitive to the refractive index near the sensing surface, and the buffer solution and pH value would not be effective in LSPR reaction because they could not change the refractive index significantly. Therefore, by coupling LSPR with CV, the LOD and SNR of the detection method could be improved by reducing the influence of electrolyte conditions and therefore attenuating background noises.

3.5. Simultaneous determination of neurotransmitters in mixed solution

Conventionally, the major advantage of spectro-electrochemistry is that, by the virtue of spectroscopy (such as Raman scattering spectroscopy), the intermediates or products, which formed during the redox reaction driven by electrochemistry, could be identified in real time. The introduction of spectroscopy into the electrochemistry, therefore, grants the spectroscopy method with reaction-orientated information and could elucidate formal reaction mechanisms (Jeanmaire and Van Duyne, 1977). In our study, the combination with CV enabled LSPR to determine the species of reactant whilst attenuate the background noises. In this section, the specificity of our coupled detection method was examined by utilizing a mixed solution of dopamine and serotonin, with ascorbic acid as the interfering substance.

Fig. 6 depicted the cyclic voltammogram and the spectro-electrochemical results of the mixed solution. In Fig. 6a, the cyclic voltammogram of mixed solution of dopamine and serotonin at 25 μmol/L, 50 μmol/L and 75 μmol/L respectively was shown. As seen from the inset, two anodic currents for dopamine and serotonin appeared respectively on the potential of 0.14 V and 0.30 V, as reported in relevant publications.

On the other hand, LSPR responses curve was obtained alone with the CV current, as shown in Fig. 6b, where the concentration of each neurotransmitter (dopamine, serotonin) was 25 μmol/L (obtained by combining the standard solution of 50 μmol/L), whilst the concentration of ascorbic acid was made as 100 μmol/L. The bathochromic shift was observed to be separated into two stages, each corresponds to the anodic current of the two neurotransmitters (i.e., the first stage of bathochromic shift was related to the signal of dopamine and the second to the signal of serotonin). By measuring the magnitude of each stage of the first bathochromic shift (dopamine: 1.61 nm, serotonin: 1.50 nm), and referring to the linearity calibration curve of LSPR responses respectively, the concentrations of dopamine and serotonin were derived as 21.29 μmol/L and 22.38 μmol/L. When compared with the actual concentration of neurotransmitters in the solution (25 μmol/L), it can be well seen that, LSPR response provided a relatively close estimation of concentration, and therefore validating the superiority of LSPR signal. Such LSPR responses were further studied by variating the concentration of neurotransmitters in the mixed solution, and the LSPR signals were obtained in Fig. 6c. As seen from the results, the LSPR responses were observed to variate in accordance with the concentration of dopamine and serotonin, confirming the causes of LSPR changes were ascribed to the redox changes of neurotransmitters. In contrast, LSPR responses in blank PBS solution was relatively small and was possibly ascribed to background noises. (See Appendix E for blank PBS detection results).

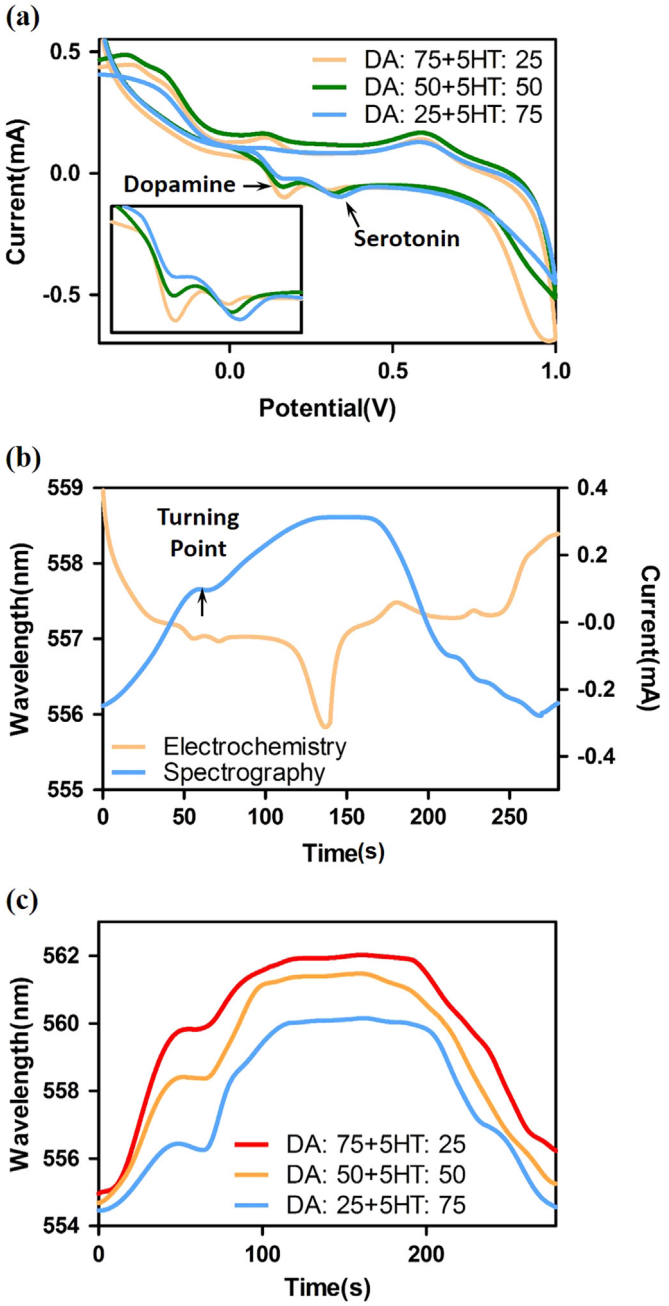

Fig. 6. Simultaneous detection of dopamine and serotonin (both 50 μmol/L) at the presence of ascorbic acid (100 μmol/L). (a) Cyclic voltammogram of the mixed solution at 25 μmol/L, 50 μmol/L and 75 μmol/L. Inset is the cyclic voltammogram at the range of 0.1 V to 0.5 V, anodic currents for dopamine and serotonin could be clearly seen as marked in the figure. (b) Spectroelectrochemical responses of the mixed solution. Corresponding to the two anodic currents, bathochromic shift of the second transmission peak was divided into two stages, separated by the turning point, and each corresponded to different neurotransmitters. (c) LSPR responses of mixed solution of dopamine and serotonin at 25 μmol/L, 50 μmol/L and 75 μmol/L. It could be observed from the figure that the LSPR responses of dopamine and serotonin variates in accordance with their concentration.

Furthermore, in order to verify the feasibility of our detection method in real samples, neurotransmitters detection was conducted in both artificial cerebrospinal fluid and brain tissue homogenates (see Appendix F and Appendix G for detection results). Also interference species like uric acid and acetylcholine were studied. Detail experiment descriptions including sample preparation, as well as detection results were included in Appendix H and Appendix I. From the results it can be observed

that although at the presence of brain tissue homogenates, the characteristic current peaks of serotonin were blurred, the LSPR responses for both dopamine and serotonin remained well-shaped. In addition, both electrochemical and LSPR signals demonstrated immunity against interferences like uric acid and acetylcholine, even at high concentrations.

It's worth mentioning that, unlike traditional unmodified glassy carbon (GC) electrodes that suffer from the existence of ascorbic acid, whose oxidation potential is very close to that of dopamine and serotonin (Thiagarajan et al., 2009; Zhu et al., 2009), our specially-designed working electrode did not show sensitivity for ascorbic acid according to our obtained results. Such immunity against ascorbic acid, might be ascribed to the electroplated AuNPs on the surface of the electrode. The negatively-charged AuNPs could repel ascorbic acid and other molecules with negative charges and attract the positively-charged neurotransmitters such as dopamine and serotonin.

4. Conclusions

In this study, a novel synchronous detection method combining cyclic voltammetry and LSPR measurement was demonstrated and utilized in neurotransmitter measurement. An AuNPs-enhanced nanosensor was developed and used as the working electrode in the electrochemical detection system, providing real-time LSPR signal of the electrode surface during CV process. Dopamine and serotonin were tested as analytes in the coupled detection system, and LSPR signals were preliminarily proved to be reliable and congruous with those of CV. Through data analysis, the CV-coupled LSPR signals demonstrated better signal-to-noise ratio compared with sole CV signals, indicating the robustness of LSPR sensing. Finally simultaneous detection of the two neurotransmitters were performed, and species as well as concentration could be determined in both direction methods.

Acknowledgments

This work was supported by the National Natural Science Foundation of China (Grant nos. 81371643, 31671007), the Zhejiang Provincial Natural Science Foundation of China for Distinguished Young Scholars (Grant no. LR13H180002), and the Collaborative Innovation Center of Traditional Chinese Medicine Health Management of Fujian Province, P.R. China.

Appendix A. Supporting information

Supplementary data associated with this article can be found in the online version at doi:10.1016/j.bios.2016.08.105.

References

Ali, S.R., Ma, Y., Parajuli, R.R., Balogun, Y., Lai, W.Y.-C., He, H., 2007. A nonoxidative sensor based on a self-doped polyaniline/carbon nanotube composite for sensitive and selective detection of the neurotransmitter dopamine. Anal. Chem. 79 (6), 2583–2587.
Arreguin, S., Nelson, P., Padway, S., Shirazi, M., Pierpont, C., 2009. Dopamine complexes of iron in the etiology and pathogenesis of Parkinson's disease. J. Inorg. Biochem. 103 (1), 87–93.
Baldrianova, L., Agrafiotou, P., Svancara, I., Jannakoudakis, A., Sotiropoulos, S., 2011. The effect of acetate concentration, solution pH and conductivity on the anodic stripping voltammetry of lead and cadmium ions at in situ bismuth-plated carbon microelectrodes. J. Electroanal. Chem. 660 (1), 31–36.
Chen, H., Kou, X., Yang, Z., Ni, W., Wang, J., 2008. Shape-and size-dependent refractive index sensitivity of gold nanoparticles. Langmuir 24 (10), 5233–5237.
Clarke, S.J., Hollmann, C., Aldaye, F.A., Nadeau, J.L., 2008. Effect of ligand density on the spectral, physical, and biological characteristics of CdSe/ZnS quantum dots. Bioconjugate Chem. 19 (2), 562–568.
Compton, R.G., Banks, C.E., 2007. Understanding Voltammetry. World Scientific.
Creese, I., Burt, D.R., Snyder, S.H., 1976. Dopamine receptor binding predicts clinical and pharmacological potencies of antischizophrenic drugs. Science 192 (4238), 481–483.
Engstrom, R.C., Weber, M., Wunder, D.J., Burgess, R., Winquist, S., 1986. Measurements within the diffusion layer using a microelectrode probe. Anal. Chem. 58 (4), 844–848.
Evans, D.H., O'Connell, K.M., Petersen, R.A., Kelly, M.J., 1983. Cyclic voltammetry. J. Chem. Educ. 60 (4), 290.
Ferreira, J., Santos, M.J., Rahman, M.M., Brolo, A.G., Gordon, R., Sinton, D., Girotto, E. M., 2008. Attomolar protein detection using in-hole surface plasmon resonance. J. Am. Chem. Soc. 131 (2), 436–437.
Gartia, M.R., Hsiao, A., Pokhriyal, A., Seo, S., Kulsharova, G., Cunningham, B.T., Bond, T.C., Liu, G.L., 2013. Colorimetric plasmon resonance imaging using nano lycurgus cup arrays. Adv. Opt. Mater. 1 (1), 68–76.
Gonon, F., Buda, M., Cespuglio, R., Jouvet, M., 1981. Voltammetry in the striatum of chronic freely moving rats: detection of catechols and ascorbic acid. Brain Res. 223 (1), 69–80.
Hafizi, S., Kruk, Z.L., Stamford, J.A., 1990. Fast cyclic voltammetry: improved sensitivity to dopamine with extended oxidation scan limits. J. Neurosci. Methods 33 (1), 41–49.
Hermans, A., Keithley, R.B., Kita, J.M., Sombers, L.A., Wightman, R.M., 2008. Dopamine detection with fast-scan cyclic voltammetry used with analog background subtraction. Anal. Chem. 80 (11), 4040–4048.
Jeanmaire, D.L., Van Duyne, R.P., 1977. Surface Raman spectroelectrochemistry: Part I. Heterocyclic, aromatic, and aliphatic amines adsorbed on the anodized silver electrode. J. Electroanal. Chem. Interfacial Electrochem. 84 (1), 1–20.
Kawagoe, K.T., Zimmerman, J.B., Wightman, R.M., 1993. Principles of voltammetry and microelectrode surface states. J. Neurosci. Methods 48 (3), 225–240.
Kawashima, S., Kanehisa, M., 2000. AAindex: amino acid index database. Nucleic Acids Res. 28 (1), 374-374.
Mahar, I., Bambico, F.R., Mechawar, N., Nobrega, J.N., 2014. Stress, serotonin, and hippocampal neurogenesis in relation to depression and antidepressant effects. Neurosci. Biobehav. Rev. 38, 173–192.
Mark, H.B., Atta, N., Ma, Y., Petticrew, K., Zimmer, H., Shi, Y., Lunsford, S., Rubinson, J., Galal, A., 1995. The electrochemistry of neurotransmitters at conducting organic polymer electrodes: electrocatalysis and analytical applications. Bioelectrochem. Bioenergy 38 (2), 229–245.
O'Neill, R.D., 1994. Microvoltammetric techniques and sensors for monitoring neurochemical dynamics in vivo. Rev. Anal. 119 (5), 767–779.
Pérez-Ruiz, T., Lozano, C.M., Tomás, V., Ruiz, E., 2007. Flow injection fluorimetric determination of L-dopa and dopamine based on a photochemical inhibition process. Microchim. Acta 158 (3–4), 299–305.
Pratuangdejkul, J., Nosoongnoen, W., Guérin, G.-A., Loric, S., Conti, M., Launay, J.-M., Manivet, P., 2006. Conformational dependence of serotonin theoretical pK a prediction. Chem. Phys. Lett. 420 (4), 538–544.
Qin, W., Wang, S., Li, J., Peng, T., Xu, Y., Wang, K., Shi, J., Fan, C., Li, D., 2015. Visualizing dopamine released from living cells using a nanoplasmonic probe. Nanoscale 7 (37), 15070–15074.
Robinson, D.L., Venton, B.J., Heien, M.L., Wightman, R.M., 2003. Detecting subsecond dopamine release with fast-scan cyclic voltammetry in vivo. Clin. Chem. 49 (10), 1763–1773.
Streeter, I., Wildgoose, G.G., Shao, L., Compton, R.G., 2008. Cyclic voltammetry on electrode surfaces covered with porous layers: an analysis of electron transfer kinetics at single-walled carbon nanotube modified electrodes. Sens. Actuators B: Chem. 133 (2), 462–466.
Sun, Y., Fei, J., Hou, J., Zhang, Q., Liu, Y., Hu, B., 2009. Simultaneous determination of dopamine and serotonin using a carbon nanotubes-ionic liquid gel modified glassy carbon electrode. Microchim. Acta 165 (3–4), 373–379.
Taylor, E.W., Duckles, S., Nelson, D.L., 1986. Dissociation constants of serotonin agonists in the canine basilar artery correlate to Ki values at the 5-HT1A binding site. J. Pharmacol. Exp. Ther. 236 (1), 118–125.
Thiagarajan, S., Tsai, T.-H., Chen, S.-M., 2009. Easy modification of glassy carbon electrode for simultaneous determination of ascorbic acid, dopamine and uric acid. Biosens. Bioelectron. 24 (8), 2712–2715.
Uutela, Pi, Karhu, L., Piepponen, P., Käenmäki, M., Ketola, R.A., Kostiainen, R., 2008. Discovery of dopamine glucuronide in rat and mouse brain microdialysis samples using liquid chromatography tandem mass spectrometry. Anal. Chem. 81 (1), 427–434.
Voegel, P.D., Zhou, W., Baldwin, R.P., 1997. Integrated capillary electrophoresis/electrochemical detection with metal film electrodes directly deposited onto the capillary tip. Anal. Chem. 69 (5), 951–957.
Wang, J., 1985. Stripping Analysis: Principles, Instrumentation, and Applications. Vch Pub.
Wang, J., 2006. Analytical Electrochemistry. John Wiley & Sons.
Wang, S., Forzani, E.S., Tao, N., 2007. Detection of heavy metal ions in water by high-resolution surface plasmon resonance spectroscopy combined with anodic stripping voltammetry. Anal. Chem. 79 (12), 4427–4432.
Wang, Z.-h, Liang, Q.-l, Wang, Y.-M, Luo, G.-A, 2003. Carbon nanotube-intercalated graphite electrodes for simultaneous determination of dopamine and serotonin in the presence of ascorbic acid. J. Electroanal. Chem. 540, 129–134.
Willets, K.A., Van Duyne, R.P., 2007. Localized surface plasmon resonance spectroscopy and sensing. Annu. Rev. Phys. Chem. 58, 267–297.

Wright-Honari, S., Marshall, E.F., Ashton, C.H., Hassanyeh, F., 1990. Estimation of human blood plasma 5-hydroxyindoleacetic acid and homovanillic acid. Biomed. Chromatogr. 4 (5), 201–204.
Wu, H.-P., Cheng, T.-L., Tseng, W.-L., 2007. Phosphate-modified TiO2 nanoparticles for selective detection of dopamine, levodopa, adrenaline, and catechol based on fluorescence quenching. Langmuir 23 (14), 7880–7885.
Wu, K., Fei, J., Hu, S., 2003. Simultaneous determination of dopamine and serotonin on a glassy carbon electrode coated with a film of carbon nanotubes. Anal. Biochem. 318 (1), 100–106.
Zhang, D., Lu, Y., Jiang, J., Zhang, Q., Yao, Y., Wang, P., Chen, B., Cheng, Q., Liu, G.L., Liu, Q., 2015. Nanoplasmonic biosensor: coupling electrochemistry to localized surface plasmon resonance spectroscopy on nanocup arrays. Biosens. Bioelectron. 67, 237–242.
Zhao, W., Brook, M.A., Li, Y., 2008. Design of gold nanoparticle-based colorimetric biosensing assays. ChemBioChem 9 (15), 2363–2371.
Zheng, X., Liu, Q., Jing, C., Li, Y., Li, D., Luo, W., Wen, Y., He, Y., Huang, Q., Long, Y.T., 2011. Catalytic gold nanoparticles for nanoplasmonic detection of DNA hybridization. Angew. Chem. Int. Ed. 50 (50), 11994–11998.
Zhou, S.Y., Zuo, H., Stobaugh, J.F., Lunte, C.E., Lunte, S.M., 1995. Continuous in vivo monitoring of amino acid neurotransmitters by microdialysis sampling with online derivatization and capillary electrophoresis separation. Anal. Chem. 67 (3), 594–599.
Zhu, S., Li, H., Niu, W., Xu, G., 2009. Simultaneous electrochemical determination of uric acid, dopamine, and ascorbic acid at single-walled carbon nanohorn modified glassy carbon electrode. Biosens. Bioelectron. 25 (4), 940–943.